



Published in final edited form as:

Biochemistry. 2009 October 27; 48(42): 10151. doi:10.1021/bi900918b.

Pyrroloquinoline Quinone Biogenesis: Demonstration that PqqE from *Klebsiella pneumoniae* is a Radical SAM Enzyme[†]

Stephen R. Wecksler[‡], Stefan Stoll[§], Ha Tran[‡], Olafur T. Magnusson^{‡, #}, Shu-pao Wu^{‡, Δ}, David King^{||}, R. David Britt[§], and Judith P. Klinman^{‡, *}

[‡]Department of Chemistry and Department of Molecular and Cell Biology, University of California, Berkeley, CA 94720

^{||}HHMI Mass Spectrometry lab at the Department of Molecular and Cellular Biology, University of California, Berkeley, CA 94720

[§]Department of Chemistry, University of California, Davis, CA 95616

Abstract

Biogenesis of pyrroloquinoline quinone (PQQ) in *Klebsiella pneumoniae* requires the expression of six genes (*pqqA-F*). One of these genes (*pqqE*) encodes a 43 kDa protein (PqqE) that plays a role in the initial steps in PQQ formation (Veletrop et al. (1995) *J. Bacteriol.* 177, 5088-5098). PqqE contains two highly conserved cysteine motifs at the N and C-termini, with the N-terminal motif comprised of a consensus sequence of CX₃CX₂C that is unique to a family of proteins known as radical S-adenosyl-L-methionine (SAM) enzymes (Sofia et al. (2001) *Nucleic Acids Res.* 29, 1097-1106). PqqE from *K. pneumoniae* was cloned into *E. coli* and expressed as the native protein and with an N-terminal His₆-tag. Anaerobic expression and purification of the His₆-tag PqqE results in an enzyme with a brownish-red hue indicative of Fe-S cluster formation. Spectroscopic and physical analyses indicate that PqqE contains a mixture of Fe-S clusters, with the predominant form of the enzyme containing two [4Fe-4S] clusters. PqqE isolated anaerobically yields active enzyme capable of cleaving SAM to methionine and 5'-deoxyadenosine in an uncoupled reaction ($k_{obs} = 0.011 \pm 0.001 \text{ min}^{-1}$). In this reaction, the 5'-deoxyadenosyl radical either abstracts a hydrogen atom from a solvent accessible position in the enzyme or obtains a proton and electron from buffer. The putative PQQ substrate PqqA has not yet been shown to be modified by PqqE, implying either that PqqA must be modified before becoming the substrate for PqqE and/or that another protein in the biosynthetic pathway is critical for the initial steps in PQQ biogenesis.

Keywords

Quinones; cofactor; biogenesis; S-adenosyl-methionine; pyrroloquinoline quinone; radicals; iron-sulfur clusters

[†]This work was supported by research grants from the National Institutes of Health (GM39296 to JPK, GM073789 to DB and F32GM080795 to SRW) and Howard Hughes Medical Institute (to DK).

*To whom correspondence should be sent: tel: 510-642-7460; fax: 510-643-6232; klinman@berkeley.edu.

[#]Present address: Decode Genetics, Sturlagata 8, IS-101 Reykjavik, Iceland.

^ΔPresent address: Department of Applied Chemistry, National Chiao Tung University, 1001 Hsueh Road, Hsinchu, Taiwan, Republic of China.

Supporting Information **Available:** Methods for the aerobic and anaerobic growth and induction of *E. coli* BL21(DE3) cells harboring the *pET24b-pqqE* plasmid, aerobic purification of PqqE, anaerobic reconstitution of PqqE with iron and sulfide ions, synthesis and purification of SAM, and a detailed description of the high resolution mass spectrometry experiments. This material is available free of charge via the Internet at <http://pubs.acs.org>.

The broad spectrum of chemical reactions catalyzed by enzymes frequently requires functional groups that are unavailable from the side chains of the 20 naturally occurring amino acids. In particular, there is a lack of electrophilic functional groups necessitating the involvement of exogenous metal ions or organic cofactors. The quino-cofactor family of enzymes contains intrinsic electrophilic centers that are derived from naturally occurring amino acids, thereby expanding the scope of amino acid side chains available within active sites of folded proteins. These cofactors arise via two fundamentally different pathways which, in the first case, involves the addition of a redox active copper ion to a folded precursor protein followed by the “self-processing” of a tyrosine side chain to trihydroxyphenylalanine quinone (TPQ) or the cross-linked lysyl tyrosine quinone (LTQ) (1). The second class of cofactors is derived from active site tryptophans and depends on an exogenous family of gene products to produce the active site tryptophanyl tryptophan quinone (TTQ) and cysteinyl tryptophan quinone (CTQ). Finally, there is the prokaryotic cofactor pyrroloquinoline quinone (PQQ), which is formed and then excised from a peptide to generate a “stand alone” cofactor. The biogenesis of both the CTQ-containing amine dehydrogenase and PQQ have been proposed to require free radical generating enzymes, specifically members of the radical *S*-adenosyl-L-methionine (SAM) enzyme family (2,3). In this report, we document the first evidence of an active radical SAM enzyme in the biogenesis pathway leading to an amino acid derived quino-cofactor.

PQQ is a non-covalently bound cofactor dominantly utilized by alcohol and sugar dehydrogenases localized in the periplasm of gram-negative bacteria (4-6). The electrons obtained upon reduction of PQQ to PQQH₂ are subsequently transferred to an electron transport chain responsible for ATP production (7). Certain bacteria, such as *E. coli*, are unable to themselves produce PQQ, and PQQ has been designated as a prokaryotic vitamin in such cases (7). The role of PQQ in mammals is much more controversial. PQQ has been found in high concentrations in breast milk, shown to be an essential nutrient for proper growth and development in mice, and even suggested to be a novel B vitamin (8-10). These observations have stoked considerable interest in its physiological function and have highlighted the importance of understanding the biosynthetic pathway *in vivo*.

Insights into the PQQ biosynthetic pathway have emerged piecemeal over the last two decades. A major breakthrough was the demonstration that PQQ is formed from the fusion of glutamate and tyrosine (Scheme 1) (11-12). This observation paralleled the discovery of genes involved in PQQ biogenesis (3,13,14). In *K. pneumoniae*, there are six genes (designated *pqqA-F*) located in the *pqq* operon (15). *pqqA* encodes a 23-residue peptide (PqqA) with a strictly conserved glutamate and tyrosine that is believed to be the substrate for PQQ biogenesis (15). PqqC catalyzes the final step in PQQ biogenesis, which is the eight-electron oxidation and ring cyclization of 3a-(2-amino-2-carboxyethyl)-4,5,-dioxo-4,5,6,7,8,9,-hexahydroquinoline-7,9-dicarboxylic acid (AHQQ) (16-17). Although no definitive functions for PqqB and PqqF have been experimentally demonstrated, sequence alignments suggest that both proteins may function as proteases. PqqD is a small 10 kDa protein that has no homology to other proteins in the protein data bank, and PqqE contains a conserved cysteine motif that is present in proteins known as radical SAM enzymes (18).

The most detailed mechanistic information in the biosynthetic pathway describes the final step for PQQ formation catalyzed by PqqC (19), with little being known about the preceding chemical steps in biogenesis. An *in vivo* study of the genes from *K. pneumoniae* suggests that PqqA, PqqD, and PqqE are critical for the first steps in PQQ biogenesis (15). We now present the first *in vitro* characterization of one of these proteins, the radical SAM enzyme PqqE. As described herein, PqqE is most homologous to the radical SAM enzyme MoaA (18 % identical and 38 % similarity to MoaA from *Mycobacterium tuberculosis*) (20). MoaA, which is involved in molybdenum cofactor biosynthesis, possesses two [4Fe-4S] clusters, one at its N-terminus and at its C-termini (21). The Fe-S cluster at the N-terminal domain provides a site for SAM

binding and activation whereas the second cluster at the C-terminus appears to play a role in anchoring and positioning of the 5'-GTP substrate. Spectroscopic and physical measurements of PqqE confirm two [4Fe-4S] clusters that display spectroscopic properties nearly identical to those found in other radical SAM enzymes. Importantly these PqqE preparations are shown to reductively cleave SAM to methionine and 5'-deoxyadenosyl radical in an uncoupled reaction, and that the enzyme is capable of multiple turnovers. These studies raise many provocative questions regarding the coupling of a radical SAM enzyme to substrate oxidation and open up, for the first time the full characterization of radical SAM enzymes in quinocofactor biogenesis.

Experimental

Materials

All chemicals and reagents were purchased from Sigma-Aldrich, Mallinckrodt, Acros, or Fisher. Chemicals and reagents were purchased at the highest purity available and used without further purification. *pET24b*, *pET28b*, and BugBuster^R were purchased from Novagen. *E. coli* BL21(DE3) and XL-1 Blue competent cells were purchased from Stratagene. All restriction enzymes (*NdeI*, *BamHI*) used for cloning reactions were purchased from New England BioLabs, calf intestinal alkaline phosphatase from Invitrogen, and high fidelity PFU polymerase and T7 DNA ligase from Roche. Bradford Assay reagents were purchased from BioRad, bovine serum albumin from Pierce, Ni²⁺-nitrilotriacetic acid (Ni-NTA) agarose resin from Qiagen, and Q-Sepharose and Sephacryl S-300 from Sigma.

Plasmids *pPH149* and *pPH151* containing the *E. coli* *IscSUA-HscBA-Fd* and *E. coli* *suf ABCDSE* genes, respectively, were generously donated by Petra Hänzelmann from the Institute for Structural Biology at the University of Würzburg, Germany. Plasmid *pBCP-165* containing the *pqq* operon from *K. pneumoniae* was originally made in the laboratory of Professor Peter W. Postma (University of Amsterdam, The Netherlands) and donated by Professor Robert Rucker from University of California at Davis. A clone containing the *sam2* gene from *E. coli* (TB1 (pUC18:*sam2*)) was generously donated by Dr. Charles Roessner from the laboratory of Prof. Ian Scott (Texas A&M University).

General Methods

All inert atmosphere work was carried out in an 855-AC-controlled atmosphere chamber from Plas-Labs, Inc. (Lansing, Michigan). For inert atmosphere work, all buffer solutions were made anaerobic by purging solutions with argon for 1 mL/min. Reagents were either prepared as anaerobic buffers or brought into the box in crystalline powder form and then reconstituted with anaerobic buffer. DNA sequencing was performed at the DNA sequencing facility at the University of California at Berkeley. N-terminal sequencing was done at the Stanford PAN facility. Iron and sulfide analyses were determined using methods described by Beinert (22-23). Protein concentrations were calculated using the Bradford Assay. UV-vis spectra were recorded on either a Hewlett-Packard 8452 diode array spectrophotometer or a Cary 50 Bio spectrophotometer. UV-visible measurements were performed in long stem quartz cuvettes (Starna) sealed with a rubber septum. PCR reactions were carried out on a PTC-200 Peltier thermal cycler (MJ Research).

Cloning of *pqqE* from *pBCP-165*—*pBCP-165* was originally generated in the laboratory of Prof. Postma at the University of Amsterdam (3). The gene sequence for the *pqq* operon from *K. pneumoniae* has been deposited in the NCBI database and used as a reference for comparing DNA and protein sequencing information. The open reading frame for *pqqE* starts at base 3023 in the operon; however, this start codon is not the typical ATG found for most bacterial genes. Position 3023 in the deposited sequence is listed as a guanine base, and was

mutated to an adenosine in order to generate the ATG start site when designing appropriate primers for the cloning of *pqqE*.

pqqE was cloned into the *NdeI* and *BamHI* restriction sites of *pET28b* (or *pET24b*) using standard cloning techniques. The following primers (obtained from Operon) were used to clone *pqqE* out of pBCP-165: 5'-CGCATTACATATGAGCCAGAGTAAACCCACCGTCAATCCG-3', 5'-CGCGGATCCTTACAGGTCCCGGGTTTGGTAGATCAGCTG-3'. Underlined bases show engineered restriction sites for *NdeI* and *BamHI*, respectively. The plasmids (named *pET28b-pqqE* and *pET24b-pqqE*) were isolated and sequenced using the T7 promoter and terminator primers, respectively.

After isolation, *pET28b-pqqE* was co-transformed into *E. coli* BL21(DE3) competent cells with either *pPH149* or *pPH151*. The bacteria were plated onto LB agar plates containing both kan (50 µg/mL) and chl (50 µg/mL) and grown at 37 °C overnight. The following day, several colonies were picked and grown in liquid LB media at 37 °C containing 50 µg/mL of both antibiotics. After several hours the bacteria had reached log phase and were quickly mixed with 50 % glycerol, immediately frozen in liquid nitrogen and stored at -80 °C until further use.

Developmental work—Initial efforts at the expression and purification of PqqE were focused on either aerobic growth of the transformed *E. coli* cells, followed by purification of enzyme from inclusion bodies and chemical reconstitution, or expression of PqqE in *E. coli* grown anaerobically and subsequent isolation of enzyme from soluble supernatants under aerobic conditions. These methods, which proved to be unsatisfactory for various reasons, are summarized under Supplemental Material.

N-terminal-His₆-tag containing PqqE—*E. coli* BL21 (DE3) cells containing *pET28b-pqqE* and *pPH151* were grown and induced under identical anaerobic growth conditions as described in Supplemental Material for anaerobic growth of *E. coli* BL21 (DE3) containing *pET24b-pqqE* with the exception that the media also contained 50 µg/mL of chl.

For the purification of His₆ tag-containing PqqE, all steps were performed under strictly anaerobic conditions in an inert atmosphere glove box. Cell pellets (cell paste yields were approximately 4 g per 10 L of LB) were brought into the glove box and lysed for 30 min with Bugbuster in 50 mM Tris (pH 7.9), 1 mM DTT, 300 mM NaCl, 10 mM Imidazole, and 5 µL of Benzonase nuclease. The lysates were loaded into anaerobic centrifuge tubes (Beckman) and cleared via centrifugation at 15,000 × *g* at 4 °C for 20 min. The lysates were then brought back into the glove box and the reddish brown supernatants loaded onto a column containing 50 mL of Ni-NTA resin equilibrated with the same buffer (column size was 12 inches long and 2.5 inches wide). The bound protein was then washed with 100 mL of loading buffer followed by two, 100 mL stepwise gradient washes containing the same buffer but with 25 mM and 50 mM imidazole, respectively. PqqE was then eluted off the column by increasing the imidazole concentration to 200 mM. The brownish red fractions were pooled and concentrated down to approximately 5 mL using a 30 kDa Amicon membrane.

After concentration, the imidazole was removed using a gel filtration PD-10 column equilibrated with 50 mM tris (pH 7.9), 1 mM DTT, 300 mM NaCl. The protein was collected off the PD-10 column and concentrated to approximately 10 mg/mL with a 30 kDa Amicon membrane. 200 µL aliquots were loaded into glass vials (Agilent) equipped with rubber caps, brought out of the glove box and immediately frozen in liquid nitrogen. The protein was stored at -80 °C until further use.

Preparation of S-adenosyl-L-methionine—The enzymatic synthesis, purification, and characterization of *S*-adenosyl-L-methionine (SAM) largely followed literature protocols (24-26). Details can be found in Supplemental Material.

Determination of enzyme activity for PqqE using LC-MS—LC-MS was performed on an Agilent LC 1100 series equipped with an HP LC/MSD electrospray ion source and quadrupole mass spectrometer. Reversed-phase HPLC was performed on a Jupiter 4 μ Proteo 90 Å 250 \times 4.60 mm C₁₈ column (Phenomenex) and the following elution conditions were used for identifying the enzymatic products of the radical SAM reaction in PqqE: Flow rate 0.4 mL/min; 0.05 % formic acid, 1.0 % acetonitrile in water for 10 min, followed by a linear gradient from 1-30 % acetonitrile over 30 min and ending with a linear gradient increase from 30-90 % acetonitrile over the next 30 min. The quadrupole mass spectrometer was operated in the positive ion mode using the scan function from *m/z* 100-1000 (fragmentor: 70, gain: 1.0, threshold: 150, step size: 0.1). The elution profiles were recorded at 215 nm and 260 nm (10 nm bandwidth and referenced at 350 nm), respectively.

Samples for LC-MS were generated as follows: a stock solution of PqqE (~125 μ M) in 50 mM Tris, 1 mM DTT, 300 mM NaCl, and 20 % glycerol at pH 7.9 was prepared anaerobically and incubated with a ten-fold excess of sodium dithionite (DT) for 10 min. 100 μ L aliquots of reduced PqqE were diluted with an equal volume of buffer and the reaction initiated by a ten-fold addition of SAM (600 μ M). The reaction was left for 2 h and then quenched by the addition of neat formic acid to give a final concentration of 5 % v/v. The samples were pelleted via centrifugation, brought out of the glove box and 80 μ L volumes injected onto the LC-MS.

Quantification of 5'-deoxyadenosine formation—High-performance liquid chromatography (HPLC) was carried out on a Beckman system equipped with a diode-array detector and operated by 32 Karat 8.0 software. The software was also used for data collection and analysis. Reversed-phase HPLC was performed on a Jupiter 4 μ Proteo 90 Å 250 \times 4.60 mm C₁₈ column. The following elution conditions were used for quantifying the time-dependent formation of 5'-deoxyadenosine: Flow rate 1 mL/min; 0.05 % formic acid, 1.0 % acetonitrile in water for 30 min, followed by a linear gradient from 1-100% acetonitrile in 10 min. Spectra were recorded at 215 nm and 260 nm, respectively. Under these conditions SAM and methionine elute in the dead time of the instrument (~ 5.0 min) and 5'-deoxyadenosine elutes at 23 min. The concentration of 5'-deoxyadenosine was determined via integration of the area under the peak and comparison to a linear calibration curve from a series of standards at known concentrations.

All assays were performed in an anaerobic chamber. For a typical assay, PqqE was prepared as a stock solution at 39 μ M in 50 mM Tris (pH 7.9), 1 mM DTT, 300 mM NaCl, 20 % glycerol, and 1 mM dithionite. The stock solution was left to incubate at room temperature for approximately 10 min, at which point SAM was added to the reaction mixture for a final concentration of 420 μ M. The samples were left to incubate for various lengths of time and quenched with neat formic acid to a final concentration of 5 %. The samples were pelleted via centrifugation and 100 μ L aliquots injected into the HPLC using the procedure outlined above.

EPR characterization—Preparation of all samples was done in an anaerobic glove box. In brief, a 1.5 mL stock solution of PqqE was prepared with 169 μ M PqqE in 50 mM Tris (pH 7.9), 1 mM DTT, 300 mM NaCl, and 20 % glycerol. The samples were cleared of precipitate at 14,000 rpm for 10 min, diluted to a final concentration of 115 μ M, loaded into EPR tubes equipped with rubber septa, brought out of the glove box and immediately frozen in liquid nitrogen. To prepare the reduced PqqE sample, the stock solution was mixed with a ten-fold excess of sodium dithionite (1.15 mM) and left to incubate for approximately 10 min before loading into the EPR tubes. The reduced samples that contained SAM were prepared in an

identical manner to the reduced PqqE sample, except a ten-fold excess of SAM (1.15 mM) was added after the 10-min incubation with dithionite. The total incubation time for the reduced PqqE with SAM was approximately 5 min.

EPR experiments were carried out at the CalEPR center at the University of California at Davis, using a Bruker ECS106 X-band spectrometer equipped with a TE₁₀₂ cavity (ER4102ST) resonating at about 9.5 GHz and an Oxford ESR900 helium cryostat with an ITC503 temperature controller. The field modulation was 1.0 mT at 100 kHz. All spectra were background corrected using a control without PqqE and SAM. Spin quantitation was done under non-saturating conditions (40K, 1mW) with the double integrals of the EPR spectra using a series of Cu²⁺-EDTA solutions between 22 μM and 177 μM for calibration.

Synthesis and purification of PqqA—PqqA (WKKPAFIDLRLGLEVTLYISNR) was synthesized on an ABI 431 synthesizer via standard Fmoc chemistry on a solid phase support. The peptide was cleaved from the PEG resin under argon using reagent K (trifluoroacetic acid, phenol, water, thioanisole, and ethanedithiol), filtered through a fritted glass funnel and precipitated into a bath of ice-cold diethylether. The precipitated peptide was centrifuged at 15,000 × *g* for 20 min at 4 °C and then washed several times with cold ether. The pellet was vacuum-dried overnight and then reconstituted with 50 % acetonitrile in water and 0.1 % trifluoroacetic acid. The reconstituted peptide was lyophilized to dryness and then stored at -20 °C until it was purified.

The crude peptide was purified via reversed phase HPLC using a semi-preparative Luna 5μ 100 Å 250 × 10.00 mm C₁₈ column (Phenomenex). The following elution conditions were used for the purification of PqqA: Flow rate 2 mL/min; 0.05 % formic acid, 1.0 % acetonitrile in water for 5 min, followed by a linear gradient from 1-15 % acetonitrile in 5 min, followed by a linear gradient from 15-65 % acetonitrile in 50 min and finishing with a wash from 65-100 % acetonitrile in 10 min. Spectra were recorded at 215 nm and 280 nm, respectively. Under these conditions, PqqA elutes at approximately 38 % acetonitrile. The fractions were analyzed via mass spectrometry and appropriate fractions pooled and lyophilized to dryness. The final yield for purified peptide was approximately 60%. A detailed description of the methods and instrumentation used for obtaining high resolution mass spectra of purified peptide and the peptide subject to reaction conditions is given in Supplemental Material.

MALDI-TOF mass spectrometry assay used to characterize enzyme-induced modifications of PqqA—Purified PqqA was brought into the glove box and anaerobically reconstituted with 50 mM Tris (pH 7.9), 1 mM DTT, 300 mM NaCl. After purification, the peptide had extremely poor solubility in water or buffer and therefore the concentration of soluble peptide in solution was determined via an estimated extinction coefficient at 280 nm of 6970 M⁻¹cm⁻¹ (estimation based on a linear combination of known extinction coefficients for aromatic residues). Saturated solutions of PqqA gave a final concentration of approximately 200 μM.

All assays were performed in an anaerobic chamber. For a typical assay, PqqE was prepared as a stock solution at 90 μM in 50 mM Tris (pH 7.9), 1 mM DTT, 300 mM NaCl, 20 % glycerol, and 1 mM dithionite. The stock solution was left to incubate at room temperature for approximately 10 min, at which point 50 μL aliquots were taken out and added to an equal volume of buffer containing a ten-fold excess of SAM (450 μM). The samples were then mixed with stoichiometric amounts of PqqA (45 μM), left to incubate for various lengths of time, and quenched with neat formic acid to a final concentration of 5 % v/v. The reactions were pelleted via centrifugation, and approximately 40 μL of sample solution were loaded onto a C₄ zip tip (Millipore) and washed several times with water. The peptide/protein mixture was then eluted

onto the MALDI plate with 80 % acetonitrile, 0.05 % formic acid, and approximately 1 mM sinapinic acid.

MALDI-TOF mass spectrometry was performed on a Voyager-DE Pro (Applied Biosystems). The samples were analyzed in positive ion reflectron mode (accelerating voltage: 20000V, grid: 75, guide wire: 0, delay time: 130 nsec, shots/spectrum: 100, mass range: 500-5000, low mass gate: 500). Calibration curves were generated using the mass spectrometry standards (Sigma) ProteoMass ACTH fragment 18-39 (2464.1989,) and insulin-oxidized B chain (3494.6513).

Results

Initial efforts at aerobic expression of PqqE

Other investigators have reported the successful expression of radical SAM enzymes under aerobic conditions (27). However, when *E. coli* cells containing the *pqqE* expression vector (*pET24b*-see Experimental section) were grown and induced under aerobic conditions PqqE was found solely in insoluble inclusion bodies. A purification scheme consisting of protein refolding followed by anion exchange and gel filtration resulted in enzyme of greater than 95 % purity (according to SDS PAGE analysis, data not shown). These preparations of PqqE were purged with argon, brought into an inert atmosphere glove box and anaerobically reconstituted in the presence of DTT with a ten-fold excess of $\text{Fe}^{2+}/\text{Fe}^{3+}$ and S^{2-} ions. After desalting the protein through a PD-10 column, the enzyme showed a red-brown hue indicative of Fe-S cluster formation.

The UV-vis spectrum of reconstituted PqqE had absorbance maxima at 390 nm and 420 nm, and labile iron and sulfide contents of 8.5 ± 0.8 moles and 6.7 ± 0.6 moles per mole of protein, respectively. The EPR spectrum (data not shown) of reconstituted PqqE appeared consistent with a $[\text{4Fe-4S}]^+$ cluster ($g = 2.05$ and 1.94); we had expected this form of the enzyme to be EPR silent due to the typical diamagnetic $[\text{4Fe-4S}]^{2+}$ oxidation state found in other radical SAM enzymes (28,29). Reduction of the enzyme with a ten-fold excess of dithionite had little effect on the EPR or the UV-vis spectrum, even in the presence of SAM. The anaerobic reconstitution of apo-PqqE with iron and sulfide ions was performed in the presence of 1 mM DTT, and we had originally suspected that the redox potential of the cluster(s) might have permitted reduction to the $[\text{4Fe-4S}]^+$ state by the excess dithiothreitol ($\epsilon^\circ = -0.33\text{V}$ at pH 7). This would be consistent with the fact that no change in the spectrum is observed upon the addition of a ten-fold excess of dithionite. It is clear from the spectral shape and g values that this species is not a $[\text{3Fe-4S}]^+$ cluster (30), but whether the species is a $[\text{4Fe-4S}]^+$ or $[\text{4Fe-4S}]^{3+}$ cluster is still unknown. Regardless, these spectral characteristics are not consistent with those found for other radical SAM enzymes and, thus, dictated a new approach toward obtaining active enzyme.

A soluble expression system was developed for PqqE by growing and inducing the cells under anaerobic conditions, eliminating the need to refold the protein. However, aerobic purification of these preparations resulted in similar physical and spectroscopic properties (after anaerobic chemical reconstitution) to that of refolded PqqE. Further, despite extensive efforts these forms of the protein failed to show activity towards SAM cleavage. Therefore, it seemed mandatory to use a strictly anaerobic expression and purification protocol, which has been shown to enhance the activity for other radical SAM enzymes (27,28,31).

Cloning, expression, and anaerobic purification of N-terminal His₆-tag containing PqqE

In the context of maintaining strictly anaerobic conditions during cell growth and purification, a His₆-tag was appended to the N-terminus of PqqE (see Experimental section). Additionally,

E. coli BL21(DE3) cells were co-transfected with vectors expressing the *E. coli* *suf* *ABCDSE* (*pPH151*) genes as well as *pqqE*, with the goal of facilitating Fe-S cluster repair and assembly (32,33). In a previously published report, *pPH151* was co-transformed with a gene encoding the radical SAM protein MOCS1A into *E. coli* BL21(DE3) cells (27) resulting in a 1.7-2.2-fold increase in soluble MOCS1A; a similar two-fold increase soluble PqqE was obtained in the present case.

The use of strictly anaerobic conditions (for growth, induction, and protein purification, see Experimental section) resulted in protein with greater than 90 % purity (Figure 1) at an average yield of 0.5-1.5 mg/L of LB media. The mobility of PqqE on a SDS gel electrophoresis is consistent with a calculated molecular weight for apo-PqqE of 44.9 kDa. There is a small impurity still present after anaerobic purification that has a molecular weight of approximately 30 kDa and has been tentatively assigned to a FK506 binding protein (FKBP)-type peptidyl-prolyl cis-trans isomerase. N-terminal sequencing of the purified protein preparation unveiled an impurity with a sequence of MKVAKDLVVS, and comparison of this sequence to that of other known sequences (in the NCBI database) provided the basis for the assignment. N-terminal sequencing also confirmed the identity of the His₆-tag containing PqqE with the N-terminus methionine removed.

Anaerobically purified PqqE has a dark brown-red color indicating the presence of Fe-S clusters. Although the enzyme is stable for days under anaerobic conditions and in the presence of DTT, it rapidly decomposes and eventually precipitates in the presence of oxygen. This form of enzyme is not amenable to anaerobic reconstitution with an excess of ferrous or sulfide ions as these treatments resulted in fast precipitation of the enzyme. The iron and sulfide contents found in the anaerobic preparations are 10.4 ± 0.9 moles and 7.0 ± 1.0 moles per monomer of protein, respectively.

Spectroscopic Characterization of PqqE

PqqE has an optical absorption spectrum (Figure 2) similar to that found for other radical SAM enzymes with absorbance maxima at 390 nm, 420 nm and a shoulder at 550 nm (27,28,31). The broad absorption spectrum undergoes complete and immediate bleaching in the presence of a ten-fold excess of sodium dithionite, and then slowly reforms upon exposure to air. The UV-vis spectrum, extinction coefficients, and iron and sulfide analyses indicate that PqqE grown and isolated anaerobically contains multiple Fe-S clusters, the nature of which was further probed via EPR.

The continuous wave X-band EPR spectrum of as-isolated PqqE, PqqE reduced with a ten-fold excess of dithionite, and reduced PqqE with a ten-fold excess of SAM are shown in Figure 3. As isolated PqqE is nearly EPR silent in the $g = 2$ region, consistent with what is expected for a diamagnetic $[4\text{Fe-4S}]^{2+}$ cluster (30). The spectrum does contain a small nearly isotropic $S = 1/2$ resonance at $g = 2.01$, similar to that found for a $[3\text{Fe-4S}]^+$ cluster (20,21). At 40 K, this signal saturates easily with a half saturation power, $P_{1/2}$, of 3 mW. Quantitation of this signal gives approximately 0.01 spins/monomer of protein, showing that this signal is due to only a minor component of the enzyme. There is also a very weak signal observable at $g = 4.3$ (data not shown) that is characteristic of adventitiously bound ferric ions (30).

When PqqE is reduced with a ten-fold excess of dithionite, new features arise in the EPR spectrum. There is a strong rhombic signal with g values 2.06, 1.96, and 1.91 (Figure 3) that have been attributed to the reduced $[4\text{Fe-4S}]^+$ species (29,30). The shape and position of these signals are nearly identical to those observed in the radical SAM enzyme pyruvate-formate lyase-activating enzyme (PFL-AE) (34), and very similar to those found for MOCS1A (27). Spin quantitation gives about 0.17 spins/monomer of protein. Unlike the oxidized enzyme, this species does not saturate at 40 K ($P_{1/2} > 200$ mW).

Interestingly, there is only a moderate change of the EPR spectrum upon the addition of SAM (Figure 3). Also, the spin quantitation shows that the number of spins is unchanged. This behavior is very different from that found for PFL-AE, where it has been demonstrated that the presence of SAM significantly changes the EPR spectrum of the reduced $[4\text{Fe-4S}]^+$ cluster (34). There has also been a report on anaerobic ribonucleotide reductase that shows a change of the axial $g = 1.96$ signal to a more rhombic one in the presence of SAM (29). The effect of SAM on the EPR spectrum of the reduced $[4\text{Fe-4S}]^+$ was further probed by measuring EPR samples without glycerol. Glycerol is known to be able to coordinate to the $[4\text{Fe-4S}]^+$ cluster inducing similar spectroscopic changes to that for SAM coordination (29). When glycerol was omitted from the samples, the EPR spectrum of the reduced enzyme looked nearly identical to that which contained glycerol (Figure 3). However, the reduced enzyme with SAM (without glycerol) looked slightly different, with the feature at $g = 2.00$ more pronounced than when both SAM and glycerol were present in the sample. There were also small changes in the signal shape at $g = 1.96$.

Demonstration of enzymatic activity for PqqE

PqqE was incubated anaerobically at room temperature with a ten-fold excess of dithionite and SAM and left for 2 h. The reaction was then quenched with formic acid and analyzed by LC-MS. A second reaction (without PqqE) was run under identical conditions as a control. In the control reaction (Figure 4A), the major species elutes immediately after the solvent front at approximately 8 min and has been assigned to *S*-adenosyl-methionine. Standards of SAM elute at an identical time and give the expected mass-to-charge ratio for the singly charged positive ion of m/z 399.5 ($\text{C}_{15}\text{H}_{23}\text{N}_6\text{O}_5\text{S}^+$). Two other peaks are observed in the control reactions at approximately 10 min (m/z 136) and 33.5 min (m/z 298.5), which are attributable to the singly charged ions of adenine ($\text{C}_5\text{H}_5\text{N}_5 + \text{H}^+$) and methylthioadenosine ($\text{C}_{11}\text{H}_{14}\text{N}_5\text{O}_3\text{S}^+$), respectively. These compounds are typical thermal decomposition products of SAM and have been observed by others (35).

The same peaks are also observed in the reaction containing PqqE, but two new features emerge from the chromatogram. The peak eluting at 8 min (assigned to SAM) has decreased in intensity and there is a new species that elutes at 28 min (see Figure 4b). This ion has an m/z of 252.4 ($\text{C}_{10}\text{H}_{13}\text{N}_5\text{O}_3 + \text{H}^+$) and is due to 5'-deoxyadenosine, as standards of 5'-deoxyadenosine elute at an identical time and give an identical mass-to-charge ratio and isotope pattern. The other product of the radical SAM reaction is methionine. Although methionine absorbs weakly at 260 nm, it can be observed when the LC-MS is monitored at 215 nm. In this case (data not shown) a large peak was observed that eluted at approximately 12 min and had an m/z of 150.2. This peak elutes at an identical time to standards of methionine and gives the expected mass-to-charge ratio and isotope pattern for the singly charged, protonated species ($\text{C}_5\text{H}_{11}\text{NO}_2\text{S} + \text{H}^+$).

PqqE is capable of undergoing multiple turnovers

Anaerobic incubation of PqqE with dithionite and SAM results in the production of methionine and 5'-deoxyadenosine. The amount of 5'-deoxyadenosine formed varied with time, and experiments were performed to determine the pseudo-first order rate constant for the reaction. In these experiments, PqqE (39 μM) was reacted with an approximate ten-fold excess of both sodium dithionite (420 μM) and SAM (420 μM) at 23 °C for various amounts of time, then quenched by the addition of formic acid and analyzed via RP-HPLC (protocols outlined in the Experimental section).

The time-dependent formation of 5'-deoxyadenosine formation is shown in Figure 5. The reaction is linear over 45 min, during which time PqqE undergoes about one turnover. The rate measured for the linear portion of this reaction was $0.417 \pm 0.019 \mu\text{M}/\text{min}$. When the enzyme

concentration was decreased two-fold (19 μM), the rate of 5'-deoxyadenosine was measured at $0.236 \pm 0.0011 \mu\text{M}/\text{min}$. These experiments clearly show an enzyme dependence of 5'-deoxyadenosine formation, and give a pseudo-first order rate constant for the uncoupled reaction of $k_{\text{obs}} = 0.011 \pm 0.001 \text{ min}^{-1}$. The amount of 5'-deoxyadenosine formation was also found to be dependent on dithionite concentration, with multiple turnovers observed only when in excess to PqqE (i.e. greater than stoichiometric amounts).

Deuterium incorporation into 5'-deoxyadenosine during turnover

PqqE was exchanged into D_2O by gel filtration over a PD-10 column and reactions initiated and analyzed in an identical procedure to that described above. The chromatograms from the reactions in D_2O are nearly identical to those shown in Figure 4B. Peaks are observed at 8 min, 12 min, and 28 min, corresponding to SAM, methionine, and 5'-deoxyadenosine, respectively. Although the retention time for the products is identical to those observed in H_2O , the mass-to-charge ratio and isotope patterns are significantly different. The mass spectrum of 5'-deoxyadenosine formed from the radical SAM reaction of PqqE in H_2O is shown in Figure 6A. The expected m/z for the singly charged, protonated form of 5'-deoxyadenosine is 252.3 ($\text{C}_{10}\text{H}_{13}\text{N}_5\text{O}_3 + \text{H}^+$). The species that elutes at 28 min has an m/z of 252.4 and its isotope pattern and elution time are identical to standards containing 5'-deoxyadenosine. When the reaction was run in D_2O , the isotope distribution for the peak eluting at 28 min (Figure 6B) shifts with the largest abundance centered at 253.4. This change in isotopic distribution indicates the incorporation of a deuterium in 5'-deoxyadenosine ($\text{C}_{10}\text{H}_{12}\text{D}_1\text{N}_5\text{O}_3 + \text{H}^+$). Controls containing 5'-deoxyadenosine were incubated in D_2O under identical conditions in the absence of PqqE and showed no evidence for deuterium incorporation in the mass spectra.

Analyses of reactions containing reduced PqqE, SAM, and PqqA

In vivo experiments done by others strongly suggest that PqqA is the substrate for PQQ biogenesis, and that both PqqA and PqqE are required for the initial steps in PQQ formation (15). PqqE isolated anaerobically contains multiple iron sulfur clusters and yields active enzyme capable of reductive cleavage of SAM. The next goal was to test whether the radical SAM activity in PqqE is coupled to the putative substrate, PqqA.

In these experiments, PqqE was anaerobically incubated with a ten-fold excess of dithionite for approximately 10 min. The protein was then mixed with a ten-fold excess of SAM, followed by the addition of stoichiometric amounts of PqqA. The addition of a large excess of peptide to protein was not possible as this caused fast precipitation of the protein. Controls containing reduced PqqE and PqqA without SAM were also run. The reactions were left for several hours, quenched by the addition of formic acid, and analyzed by mass spectrometry.

Confirmation of the intact peptide after HPLC purification was achieved via high resolution mass spectrometry (calculated m/z : 2631.49, found ($\text{M} + \text{H}^+$) m/z : 2632.52). When PqqA was incubated with reduced PqqE and SAM, the mass-to-charge ratio found via MALDI-TOF mass spectrometry after reaction (data not shown) was determined to be m/z 2632.4 ($\text{M} + \text{H}^+$). The spectrum revealed no modifications of PqqA and no differences between the control peptides and that for PqqA subjected to reaction conditions. Varying amounts of reducing agent, SAM, PqqE, PqqA, and time also resulted in nearly identical mass spectra. The reactions were also analyzed via LC-MS and SDS-PAGE and no new peaks were observed in the chromatograms or gels. Finally, high resolution mass spectrometry confirmed the identity of the intact peptide after reaction and failed to show any change in the mass-to-charge ratio before and after reaction. Although these reaction mixtures failed to show any modifications of PqqA, the products of the radical SAM reaction were still observed. The amount of 5'-deoxyadenosine formed in these reactions was also quantified, and was similar to that measured without the peptide present.

Discussion

The UV-vis spectrum, labile iron and sulfide analyses, and EPR spectra have provided a good framework to characterize the nature of the Fe-S clusters present in PqqE. PqqE has strong absorption bands in the visible region with absorbance maximum at 390 nm, 420 nm and a shoulder at 550 nm, which rapidly and completely bleach in the presence of dithionite. The extinction coefficient at 420 nm is about 33,000 M⁻¹cm⁻¹, more similar to what could be expected for 2 [4Fe-4S] clusters ([4Fe-4S]²⁺ $\epsilon_{410} \sim 15,000$ M⁻¹cm⁻¹) as opposed to a [4Fe-4S]²⁺ and a [2Fe-2S]²⁺ ([2Fe-2S]²⁺ $\epsilon_{410} \sim 8,000$ -10,000 M⁻¹cm⁻¹) (36). The iron and sulfide analyses from these preparations were determined to be 10.4 ± 0.9 moles and 7.0 ± 1.0 moles per monomer of protein, respectively. These results implicate the presence of two [4Fe-4S] centers as has been reported for MOCS1A (27). Alignment of the sequence for PqqE from *K. pneumoniae* with gene sequences for *pqqE* from other sources indicates that the presence of two [4Fe-4S]²⁺ clusters is to be expected in all cases (Figure 7). The origin of the excess labile iron remains unresolved, and may be a consequence of a weak binding iron to the N-terminal His₆ domain. However, the possibility that the excess iron is part of a mononuclear iron site, or plays some type of structural role in PqqE, cannot be ruled out from the current data.

Continuous wave X-band EPR of PqqE isolated anaerobically is consistent with the hypothesis that the as-isolated enzyme primarily contains two diamagnetic [4Fe-4S]²⁺ clusters. The presence of a small axial signal at g = 2.01 (spin = 0.01/monomer) has been attributed in other radical SAM enzymes to a [3Fe-4S]⁺ cluster (29). The small signal at g = 4.3 (data not shown) for PqqE in the oxidized enzyme is consistent with what would be expected for adventitiously bound ferric iron (30). It has been previously demonstrated that gentle oxidation of the [4Fe-4S]²⁺ in radical SAM enzymes yields a [3Fe-4S]⁺ cluster, which can be anaerobically reconstituted with iron in the presence of dithiothreitol to form a [4Fe-4S]²⁺ cluster (29,37). After reduction of PqqE with dithionite, both the g = 4.3 signal and the g = 2.01 signal disappear and a new rhombic spectrum with g values at 2.06, 1.96, and 1.91 appears (spin = 0.17/monomer). The shape and g values are nearly identical to that for some other radical SAM enzymes and are consistent with a reduced [4Fe-4S]⁺ cluster (27-29). We believe that the as-isolated enzyme contains mostly two diamagnetic [4Fe-4S]²⁺ clusters and a small percentage of [3Fe-4S]⁺ clusters, presumably formed as a side product during protein purification. In analogy to that found for anaerobic ribonucleotide reductase activase (29) and PFL-AE (37), reduction with dithionite in the presence of endogenous iron results in the conversion of the [3Fe-4S]⁺ cluster to [4Fe-4S]²⁺ cluster, followed by further reduction to [4Fe-4S]⁺ cluster. Although we propose that the loss of the g = 4.3 and 2.01 spectral changes upon reduction is due to the conversion of small amounts of [3Fe-4S]⁺ to the final [4Fe-4S]⁺ cluster, we cannot rule out the conversion of some unspecified paramagnetic species to a diamagnetic form.

EPR has also been used as a valuable tool to probe SAM coordination to the reduced cluster (25). The binding of SAM was investigated in the absence and presence of glycerol, as glycerol has been previously shown to bind to the reduced [4Fe-4S]⁺ cluster and induce similar spectral changes to that of the binding of SAM (29). When glycerol was omitted, there are small perturbations in the EPR spectrum in the presence of SAM with the feature at g = 2.00 becoming more pronounced and the g = 1.96 changing shape. This indicates that the g = 2.00 signal might be part of a rhombic minority species with g values of 2.00, about 1.95 and 1.92. When SAM was added to reduced PqqE in the presence of glycerol, only small perturbations in the EPR spectrum were observed with the shape and g values nearly identical to those without SAM (see Figure 3). These results suggest that either SAM is not coordinated to the [4Fe-4S]⁺ cluster or it is coordinated only weakly. Whether this species is chemically relevant is unclear.

The spectroscopic and physical measurements described above indicate that anaerobically purified PqqE contains multiple Fe-S clusters, with the predominant form of the isolated enzyme containing two $[4\text{Fe-4S}]^{2+}$ clusters. The EPR and UV-vis spectra suggested that at least one of the clusters would be redox active with characteristics similar to that found for other radical SAM enzymes. The role of the second cluster is still unclear, but in analogy to that for MOCS1A, it may play a role in positioning the substrate for H-atom abstraction.

When PqqE was anaerobically incubated with an excess of SAM and dithionite, methionine and 5'-deoxyadenosine were formed as products of the enzymatic reaction (Figure 4). The cleavage of SAM to methionine and 5'-deoxyadenosyl radical is energetically unfavorable (bond dissociation energy for C-S of 60 kcal mol^{-1}) and is only possible via enzymatic activation (Scheme 2) (38-39). This radical is highly reactive and generally initiates the next step in catalysis via H-atom abstraction from a substrate. We have thoroughly looked for the presence of stable organic radicals in PqqE reaction mixtures via EPR without success. Therefore, the production of methionine and 5'-deoxyadenosine is concluded to derive from an "uncoupled reaction", whereby the generation of the 5'-deoxyadenosyl radical obtains a proton and electron from buffer sources to form 5'-deoxyadenosine. When reaction was run in D_2O and the reaction mixtures analyzed via LC-MS, an increase of one mass unit in the mass-to-charge ratio of 5'-deoxyadenosine (Figure 6) indicates that solvent-derived deuterium has been incorporated into the product.

The quenching of the 5'-deoxyadenosyl radical to form 5'-deoxyadenosine could occur through two different mechanisms: 1. H-atom abstraction from the protein followed by fast outersphere electron transfer to the protein-derived radical, or, 2. Reduction of the 5'-deoxyadenosyl radical by dithionite to the corresponding carbanion followed by rapid proton abstraction from the solvent. Although no organic radicals were observed in the EPR, the first mechanism can't be ruled out because outer sphere electron transfer to the protein derived radical may be so fast that it is undetectable via EPR under our assay conditions; further, H-atom abstraction from a solvent exchangeable position on PqqE would lead to the same deuterated product as direct proton transfer from solvent. The "uncoupled" production of 5'-deoxyadenosine in several other radical SAM enzymes has been observed before (40,41), but to our knowledge this is the first example of an uncoupled radical SAM reaction that leads to the incorporation of a solvent deuterium into 5'-deoxyadenosine. This may be suggestive of a solvent accessible amino acid residue in the active site of PqqE that is not shared with other radical SAM enzymes. At this juncture we are not sure how the radical is quenched, but the aggregate experiments show that a 5'-deoxyadenosyl intermediate is formed from reductive cleavage of SAM by PqqE, and are consistent with the proposed mechanism for radical SAM enzymes (38,39). The fact that deuterium incorporation is only approximately 50 % is attributable to incomplete buffer exchange in PqqE (see Experimental section) and dilution of D_2O with protiated glycerol added at a mole ratio of 8 % to reaction mixtures.

The amount of 5'-deoxyadenosine formed from the uncoupled radical SAM reaction in PqqE varied with time, undergoing multiple turnovers in the course of several hours. Furthermore, decreasing the enzyme concentration two-fold caused the rate of 5'-deoxyadenosine to decrease by a factor of two, clearly indicating an enzyme dependence on 5'-deoxyadenosine formation. The rate for the production of 5'-deoxyadenosine was linear for approximately 45 min, and during this time period $k_{\text{obs}} = 0.011 \pm 0.001 \text{ min}^{-1}$. Although this rate constant seems quite slow for an enzymatic reaction, the uncoupled rate is only approximately six times slower than that for single turnover rate constants of biotin synthase (0.07 min^{-1}) (42), $10\times$ slower than that for lipoyl synthase (0.175 min^{-1}) (43), and approximately thirty times slower than AtsB (0.38 min^{-1}) (31). This rate is only about six times slower when compared to the rate-limiting step for TPQ biogenesis ($k_{\text{bio}} = 0.08 \text{ min}^{-1}$) (44), indicating that the turnover rate is at least comparable with those found for the formation of other quinone cofactors.

We have proceeded on the premise that PqqE catalyzes the first step in PQQ biogenesis, thought to be the linking of the amino acid side chains of glutamate and tyrosine in PqqA. Previous *in vivo* labeling experiments demonstrated PQQ was formed from the fusion of glutamate and tyrosine, also providing evidence for how these amino acids are linked together (see Scheme 1) (11,12). A carbon-carbon bond is formed between the C9 of glutamate and C9a of tyrosine. It seems likely that the radical SAM enzyme could catalyze this step since the large activation energy needed to break the aromaticity of the tyrosine ring could be overcome by formation of a glutamate radical generated via H-atom abstraction by the 5'-deoxyadenosyl radical.

PqqA was tested as a substrate for PqqE by incubating the enzyme with varying amounts of SAM, dithionite, and PqqA. For these reactions, the enzyme needed to be stabilized with glycerol and PqqA slowly titrated into the reaction mixtures due to significant protein precipitation problems. Reactions were also attempted with a small amount of ethanol or denaturant to circumvent potential peptide aggregation. The reactions were left for various periods of time and then analyzed via MALDI-TOF mass spectrometry, LC-MS, SDS PAGE, EPR, and high-resolution mass spectrometry. Under all conditions, no modifications of the peptide or (radical) intermediates were observed even though the uncoupled reaction products (methionine and 5'-deoxyadenosine) were still detected. Furthermore, there were no new peaks observed in the EPR, LC-MS traces or bands in the SDS PAGE analyses. The reaction mixtures were also exposed to molecular oxygen after anaerobic incubation, on the premise that O₂ may play a role in trapping radical intermediates and driving the reaction toward products. However, these experiments failed to show any new products or modifications of PqqA. Experiments performed with glutamate and tyrosine as potential substrates for PqqE also failed to show any new products.

The fact that no modifications of PqqA have been observed may be due to lack of sensitivity of detection (for instance if only a very small amount of product were formed), or perhaps a reversible cleavage of SAM with an equilibrium that favors the reactants. Experiments are under way to test these hypotheses using spin-trapping agents and also utilizing radiolabeled [2,3,5'-³H]-SAM to look for tritium scrambling into the peptide.

Alternatively, other proteins in the PQQ biosynthetic pathway may be necessary for the initial steps in PQQ biogenesis. One possible candidate is PqqD, a gene product with no known homology to any annotated protein. PqqA may also need to be modified by another gene product in the *pqq* operon prior to reaction with PqqE. One important question that we would like to resolve is: what chemical step happens first, the cross-linking of PqqA or the hydroxylation of the conserved tyrosine? Veletrop et al. have demonstrated that molecular oxygen is critical for PQQ biogenesis (15), and it is reasonable to suggest that the hydroxylation of the tyrosine in PqqA occurs via activation of molecular oxygen. We had initially thought that PqqE may be responsible for both of these steps, however, we have yet to observe this type of unprecedented radical SAM chemistry.

It has been recently demonstrated in TTQ biogenesis that mutation of critical residues in the *mauG* gene results in the formation of a stable intermediate that does not have the tryptophan-tryptophan cross-link nor the quinone moiety, but does contain a mono-hydroxylated tryptophan (45-47). Incubation of the mono-hydroxylated intermediate with active MauG and either hydrogen peroxide or oxygen with reducing equivalents results in tryptophan-tryptophan cross-linking and concomitant formation of the quinone (48-50). In analogy to TTQ biosynthesis, we believe that hydroxylation of the tyrosine may occur before cross-linking PqqA, after which PqqE catalyzes the cross-linking via a radical mechanism. Ongoing experiments in this laboratory are aimed at oxidatively modifying the conserved tyrosine in PqqA, with the goal of assessing whether such derivations of PqqA are capable of entering into reaction with PqqE.

Supplementary Material

Refer to Web version on PubMed Central for supplementary material.

Acknowledgments

We thank Prof. Robert Rucker for the donation of the plasmid *pBCP-165* containing the *pqq* operon, Dr. Petra Hänzelmann for the donation of plasmids *pPH149* and *pPH151* containing the *E. coli* *IscSUA-HscBA-Fd* and *E. coli* *suf ABCDSE* genes, respectively, and Dr. Charles Roessner for a clone containing the *sam2* gene from *E. coli* (TB1 (pUC18:*sam2*)). We would also like to thank Dr. Junko Yano for help with preliminary EPR measurements, Dr. Tony Iavarone for obtaining high resolution mass spectra of peptides, and Ms. Mae Tulfo for help preparing the manuscript.

References

1. Klinman JP. How many ways to craft a cofactor? Proc Natl Acad Sci 2001;98:14766–14768. [PubMed: 11752422]
2. Ono K, Okajima T, Tani M, Kuroda S, Sun D, Davidson VL, Tanizawa K. Involvement of a Putative [Fe-S]-cluster-binding Protein in the Biogenesis of Quinohemoprotein Amine Dehydrogenase. J Biol Chem 2006;281:13672–13684. [PubMed: 16546999]
3. Meulenberg JJM, Sellink E, Riegman NH, van Kleef M, Postma PW. Nucleotide sequence and structure of the *Klebsiella pneumoniae pqq* operon. Mol Gen Genet 1992;232:284–294. [PubMed: 1313537]
4. Anthony C, Zatman LJ. The microbial oxidation of methanol: The prosthetic group of alcohol dehydrogenase of *Pseudomonas* sp. M27; a new oxidoreductase prosthetic group. Biochem J 1967;104:953–959. [PubMed: 6058112]
5. Salisbury SA, Forrest HS, Cruse WBT, Kennar O. A novel coenzyme from bacterial primary alcohol dehydrogenases. Nature 1979;280:843–844. [PubMed: 471057]
6. Duine JA, Frank J, van Zeeland JK. Glucose dehydrogenase from *Acinetobacter calcoaceticus*. FEBS Lett 1979;108:443–446. [PubMed: 520586]
7. Goodwin, PM.; Anthony, C. The Biochemistry, Physiology and Genetics of PQQ and PQQ-containing Enzymes. In: Poole, RK., editor. Advances in Microbial Physiology. Vol. 40. Elsevier; Amsterdam: 1998. p. 1-80.
8. Mitchell AE, Jones AD, Mercer RS, Rucker RB. Characterization of pyrroloquinoline quinone amino acid derivatives by electrospray ionization mass spectrometry and detection in human milk. Anal Biochem 1999;269:317–325. [PubMed: 10222004]
9. Killgore J, Smidt C, Duich L, Romero-Chapman N, Tinker D, Reiser K, Melko M, Hyde D, Rucker RB. Nutritional importance of pyrroloquinoline quinone. Science 1989;245:850–852. [PubMed: 2549636]
10. Kasahara T, Kato T. A new redox-cofactor vitamin for mammals. Nature 2003;422:832. [PubMed: 12712191]
11. Houck DR, Hanners JL, Unkefer CJ. Biosynthesis of pyrroloquinoline quinone. 1. Identification of a biosynthetic precursor using ¹³C labeling and NMR spectroscopy. J Am Chem Soc 1988;110:6920–6921.
12. Houck DR, Hanners JL, Unkefer CJ. Biosynthesis of pyrroloquinoline quinone. 2. Biosynthetic assembly from glutamate and tyrosine. J Am Chem Soc 1991;113:3162–3166.
13. Toyama H, Chistoserdova L, Lidstrom ME. Sequence analysis of *pqq* genes required for biosynthesis of pyrroloquinoline quinone in *Methylobacterium extorquens* AM1 and the purification of a biosynthetic intermediate. Microbiology 1997;143:595–602. [PubMed: 9043136]
14. Goosen N, Horsman HPA, Huinen RGM, Putte VDP. *Acinetobacter calcoaceticus* genes involved in biosynthesis of the coenzyme pyrroloquinoline-quinone: nucleotide sequence and expression in *Escherichia coli* K-12. J Bacteriol 1989;171:447–455. [PubMed: 2536663]
15. Velterop JS, Sellink E, Meulenberg JJM, Bulder DS, Postma PW. Synthesis of pyrroloquinoline quinone *in vivo* and *in vitro* and detection of an intermediate in the biosynthetic pathway. J Bacteriol 1995;177:5088–5098. [PubMed: 7665488]

16. Magnusson OT, Toyama H, Saeki M, Schwarzenbacher R, Klinman JP. The structure of a biosynthetic intermediate of pyrroloquinoline quinone (PQQ) and elucidation of the final step of PQQ biogenesis. *J Am Chem Soc* 2004;126:5342–5343. [PubMed: 15113189]
17. Toyama H, Fukumoto J, Saeki M, Matsushita K, Adachi O, Lidstrom ME. PqqC/D, which converts a biosynthetic intermediate to pyrroloquinoline quinone. *Biochem Biophys Res Commun* 2002;299:268–272. [PubMed: 12437981]
18. Sofia HJ, Chen G, Hetzler BG, Reyes-Spindola JF, Miller NE. Radical SAM, a novel protein superfamily linking unresolved steps in familiar biosynthetic pathways with radical mechanisms: functional characterization using new analysis and information visualization methods. *Nucleic Acids Res* 2001;29:1097–1106. [PubMed: 11222759]
19. Magnusson OT, Toyama H, Saeki M, Rojas A, Reed JC, Liddington RC, Klinman JP, Schwarzenbacher R. Quinone biogenesis: Structure and mechanism of PqqC, the final catalyst in the production of pyrroloquinoline quinone. *Proc Natl Acad Sci* 2004;101:7913–7918. [PubMed: 15148379]
20. Menendez C, Igloi G, Henninger H, Brandsch R. A pAO-1-encoded molybdopterin cofactor gene (*moaA*) of *Arthrobacter nicotinovorans*: characterization and site-directed mutagenesis of the encoded protein. *Arch Microbiol* 1995;164:142–151. [PubMed: 8588735]
21. Hänzelmann P, Schindelin H. Binding of 5'-GTP to the C-terminal FeS cluster of the radical S-adenosylmethionine enzyme MoaA provides insights into its mechanism. *Proc Natl Acad Sci* 2006;103:6829–6834. [PubMed: 16632608]
22. Beinert H. Micro methods for the quantitative determination of iron and copper in biological material. *Methods Enzymol* 1978;54:435–445. [PubMed: 732579]
23. Beinert H. Semi-micro methods for analysis of labile sulfide and of labile sulfide and sulfane sulfur in unusually stable iron-sulfur proteins. *Anal Biochem* 1983;131:373–378. [PubMed: 6614472]
24. Park J, Tai J, Roessner CA, Scott AI. Enzymatic synthesis of S-adenosyl-L-methionine on the preparative scale. *Bioorganic and Medicinal Chemistry* 1996;4:2179–2185. [PubMed: 9022980]
25. Walsby CJ, Hong W, Broderick WE, Cheek J, Ortillo D, Broderick JB, Hoffman BM. Electron-nuclear double resonance spectroscopic evidence that S-adenosylmethionine binds in contact with the catalytically active [4Fe-4S]⁺ cluster of pyruvate formate-lyase activating enzyme. *J Am Chem Soc* 2002;124:3143–3151. [PubMed: 11902903]
26. Shapiro SK, Ehniger DJ. Methods for analysis and preparation of adenosylmethionine and adenosylhomocysteine. *Anal Biochem* 1966;15:323–333. [PubMed: 4289755]
27. Hänzelmann P, Hernández HL, Menzel C, Garcia-Serres R, Huynh BH, Johnson MK, Mendel RR, Schindelin H. Characterization of MOCS1A, and oxygen-sensitive iron-sulfur protein involved in human molybdenum cofactor biosynthesis. *J Biol Chem* 2004;279:34721–34732. [PubMed: 15180982]
28. Hernández HL, Pierrel F, Elleingand E, García-Serres R, Huynh BH, Johnson MK, Fontecave M, Atta M. MiaB, a bifunctional radical-S-adenosylmethionine enzyme involved in thiolation and methylation of tRNA, contains two essential [4Fe-4S] clusters. *Biochemistry* 2007;46:5140–5147. [PubMed: 17407324]
29. Lim A, Gräslund A. Electron paramagnetic resonance evidence for a novel interconversion of [3Fe-4S]⁺ and [4Fe-4S]⁺ clusters with endogenous iron and sulfide in anaerobic ribonucleotide reductase activase *in vitro*. *J Biol Chem* 2000;275:12367–12373. [PubMed: 10777518]
30. Beinert H, Kennedy MC, Stout CD. Aconitase as iron-sulfur protein, enzyme, and iron-regulatory protein. *Chem Rev* 1996;96:2335–2373. [PubMed: 11848830]
31. Grove TL, Lee KH, St. Clair J, Krebs C, Booker SJ. *In vitro* characterization of AtsB, a radical SAM formylglycine-generating enzyme that contains three [4Fe-4S] clusters. *Biochemistry* 2008;47:7523–7538. [PubMed: 18558715]
32. Takahashi Y, Tokumoto U. A third bacterial system for the assembly of iron-sulfur clusters with homologs in archaea and plastids. *J Biol Chem* 2002;277:28380–28383. [PubMed: 12089140]
33. Nachin L, Loiseau L, Expert D, Barras F. SufC: an unorthodox cytoplasmic ABC/ATPase required for [Fe-S] biogenesis under oxidative stress. *EMBO* 2003;22:427–437.

34. Walsby CJ, Ortillo D, Yang J, Nnyepi MR, Broderick WE, Hoffman BM, Broderick JB. Spectroscopic approaches to elucidating novel iron-sulfur chemistry in the “radical-SAM” protein superfamily. *Inorg Chem* 2005;44:727–741. [PubMed: 15859242]
35. Hoffman JL. Chromatographic analysis of the chiral and covalent instability of S-adenosyl-L-methionine. *Biochemistry* 1986;25:4444–4449. [PubMed: 3530324]
36. Dailey HA, Finnegan MG, Johnson MK. Human ferrochelatase is an iron-sulfur protein. *Biochemistry* 1994;33:403–407. [PubMed: 8286370]
37. Krebs C, Broderick WE, Henshaw TF, Broderick JB, Huynh BH. Coordination of adenosylmethionine to a unique iron site of the [4Fe-4S] cluster of pyruvate formate lyase-activating enzyme: A Mössbauer spectroscopic study. *J Am Chem Soc* 2002;124:912–913. [PubMed: 11829592]
38. Frey PA. Radical mechanisms of enzyme catalysis. *Annu Rev Biochem* 2001;70:121–148. [PubMed: 11395404]
39. Frey PA, Magnusson OT. S-adenosylmethionine: A wolf in sheep's clothing, or a rich man's adenosylcobalamin? *Chem Rev* 2003;103:2129–2148. [PubMed: 12797826]
40. Ollagnier-de Choudens S, Sanakis Y, Hewiston KS, Roach P, Munck E. Reductive of S-adenosylmethionine by biotin synthase from *Escherichia coli*. *J Biol Chem* 2002;277:13449–13454. [PubMed: 11834738]
41. Farrar CE, Jarrett JT. Protein Residues that Control the Reaction Trajectory is S-Adenosylmethionine Radical Enzymes: Mutagenesis of Asparagine 153 and Aspartate 155 in *Escherichia coli* Biotin Synthase. *Biochemistry* 2009;48:2448–2458.
42. Ugulava NB, Gibney BR, Jarrett JT. Iron-sulfur cluster interconversions in biotin synthase: Dissociation and reassociation of iron during conversion of [2Fe-2S] to [4Fe-4S] clusters. *Biochemistry* 2000;39:5206–5214. [PubMed: 10819988]
43. Cicchillo RM, Iwig DF, Jones AD, Nesbitt NM, Baleanu-Gogonea C, Souder MG, Tu L, Booker SJ. Lipoyl synthase requires two equivalents of S-adenosyl-L-methionine to synthesize one equivalent of lipoic acid. *Biochemistry* 2004;43:6378–6386. [PubMed: 15157071]
44. Schwartz B, Dove JE, Klinman JP. Kinetic analysis of oxygen utilization during cofactor biogenesis in a copper-containing amine oxidase from yeast. *Biochemistry* 2000;39:3699–3707. [PubMed: 10736169]
45. Pearson AR, Jones LH, Higgins L, Ashcroft AE, Wilmot CM, Davidson VL. Understanding quinone cofactor biogenesis in methylamine dehydrogenase through novel cofactor generation. *Biochemistry* 2003;42:3224–3230. [PubMed: 12641453]
46. Pearson AR, De La Mora-Rey T, Graichen ME, Wang Y, Jones LH, Marimanikkupam S, Agger SA, Grimsrud PA, Davidson VL, Wilmot CM. Further insights into quinone cofactor biogenesis: Probing the role of *mauG* in methylamine dehydrogenase tryptophan tryptophylquinone formation. *Biochemistry* 2004;43:5494–5502. [PubMed: 15122915]
47. Pearson AR, Marimanikkupam S, Li X, Davidson VL, Wilmot CM. Isotope labeling studies reveal the order of oxygen incorporation into the tryptophan tryptophylquinone cofactor of methylamine dehydrogenase. *J Am Chem Soc* 2006;128:12416–12417. [PubMed: 16984182]
48. Wang Y, Graichen ME, Liu A, Pearson AR, Wilmot CM, Davidson VL. MauG, a novel diheme protein required for tryptophan tryptophylquinone biogenesis. *Biochemistry* 2003;42:7318–7325. [PubMed: 12809487]
49. Wang Y, Li X, Jones LH, Pearson AR, Wilmot CM, Davidson VL. MauG-dependent in vitro biosynthesis of tryptophan tryptophylquinone in methylamine dehydrogenase. *J Am Chem Soc* 2005;127:8258–8259. [PubMed: 15941239]
50. Li X, Jones LH, Pearson AR, Wilmot CM, Davidson VL. Mechanistic possibilities in MauG-dependent tryptophan tryptophylquinone biosynthesis. *Biochemistry* 2006;45:13276–13283. [PubMed: 17073448]

Abbreviations

PQQ	pyrroloquinoline quinone
SAM	S-adenosyl-L-methionine

Fe-S cluster	iron-sulfur cluster
TPQ	trihydroxyphenylalanine quinone
LTQ	lysyl tyrosine quinone
TTQ	tryptophanyl tryptophan quinone
CTQ	cysteine tryptophan quinone
<i>E. coli</i>	<i>Escherichia coli</i>
<i>K. pneumoniae</i>	<i>Klebsiella pneumoniae</i>
NCBI	National Center for Biotechnology Information
DTT	dithiothreitol
PCR	polymerase chain reaction
LB media	Luria-Bertani media
amp	ampicillin
kan	kanamycin
chl	chloramphenicol
LC-MS	liquid chromatography-mass spectrometry
DT	sodium dithionite
HPLC	high performance liquid chromatography
EPR	electron paramagnetic resonance
EDTA	ethylenediaminetetraacetic acid
Fmoc	fluorenylmethyloxycarbonyl
PEG	polyethylene glycol
MALDI-TOF	matrix-assisted laser desorption ionization-time of flight
PFL-AE	pyruvate-formate lyase-activating enzyme
SDS-PAGE	sodium dodecyl sulfate polyacrylamide gel electrophoresis
5'-dA	5'-deoxyadenosine

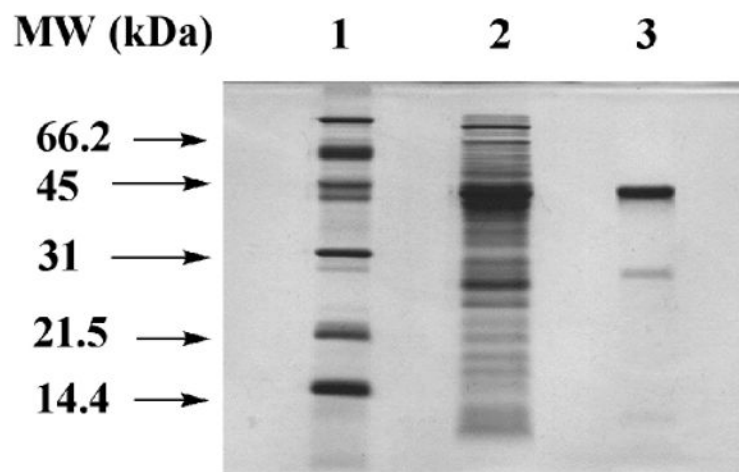


Figure 1.
SDS-PAGE analysis of purified N-terminal His₆-tag containing PqqE. Lane 1: protein marker.
Lane 2: crude PqqE. Lane 3: purified PqqE.

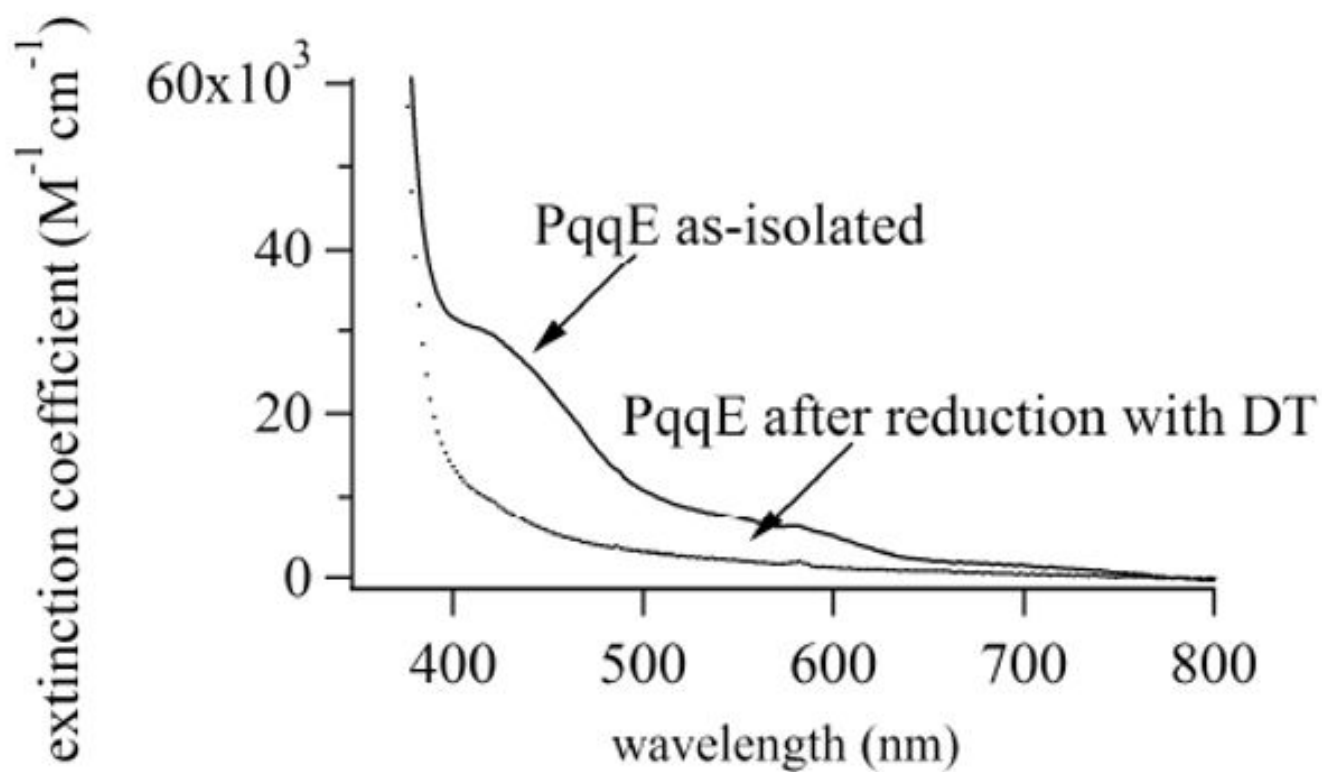


Figure 2. UV-vis spectrum of purified PqqE before (solid line) and after (dotted line) reduction with dithionite (DT).

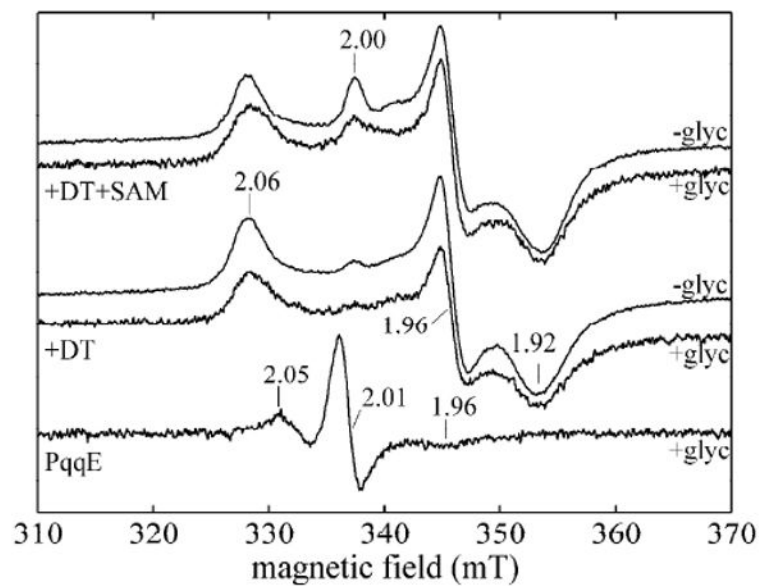


Figure 3.

Continuous Wave X-band EPR of as-isolated PqqE, PqqE (with and without glycerol) reduced with dithionite (DT), and reduced PqqE with a ten-fold excess of SAM (with and without glycerol). The total incubation for the SAM sample was less than 5 min. EPR conditions: temperature 40 K; microwave power 6.3 mW; microwave frequency 9.480 GHz.

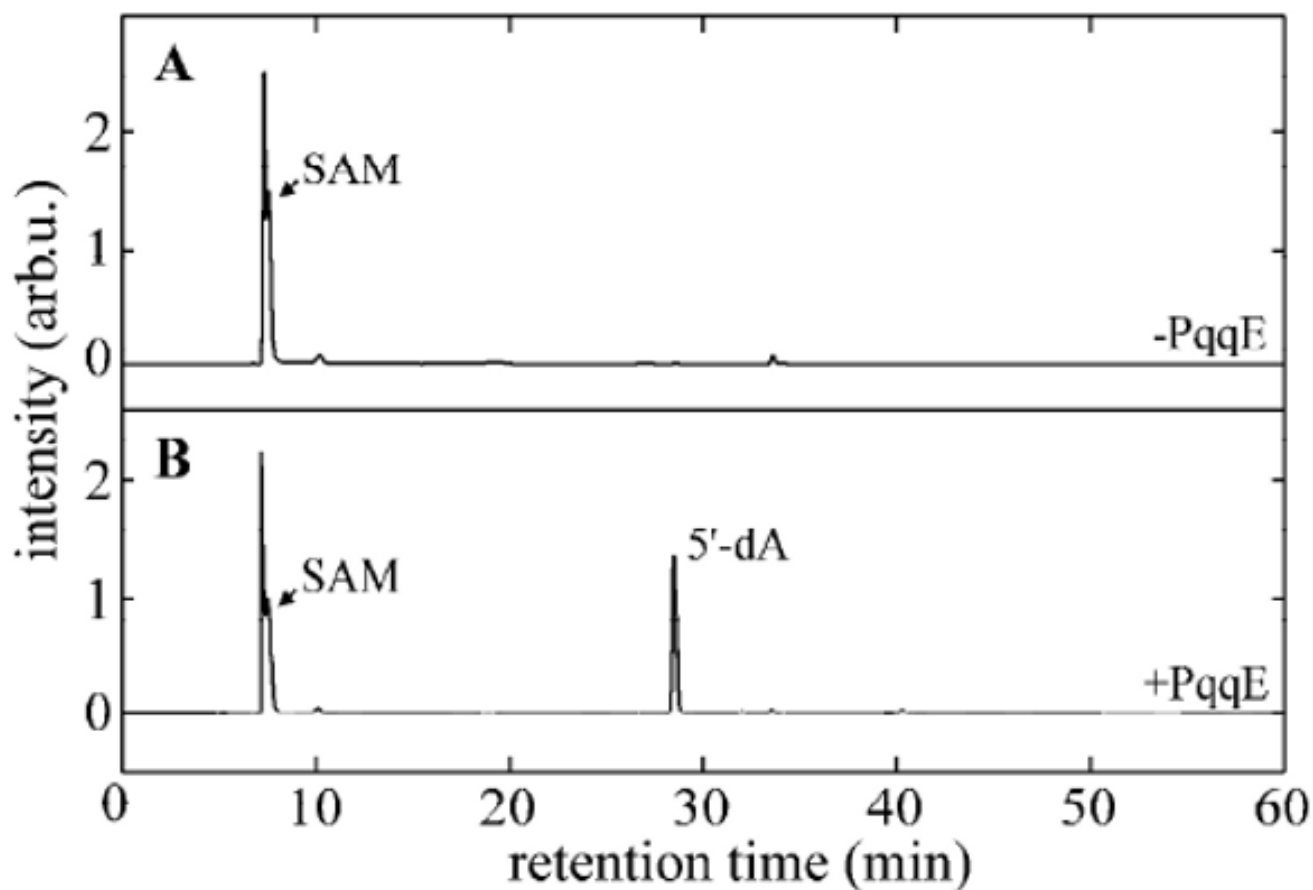


Figure 4. LC-MS analyses of the reaction products from *in vitro* activation of PqqE with dithionite and SAM. A. LC-MS elution profile (monitored at 260 nm) of control without PqqE B. LC-MS elution profile of anaerobic reaction mixture containing PqqE, SAM, and dithionite.

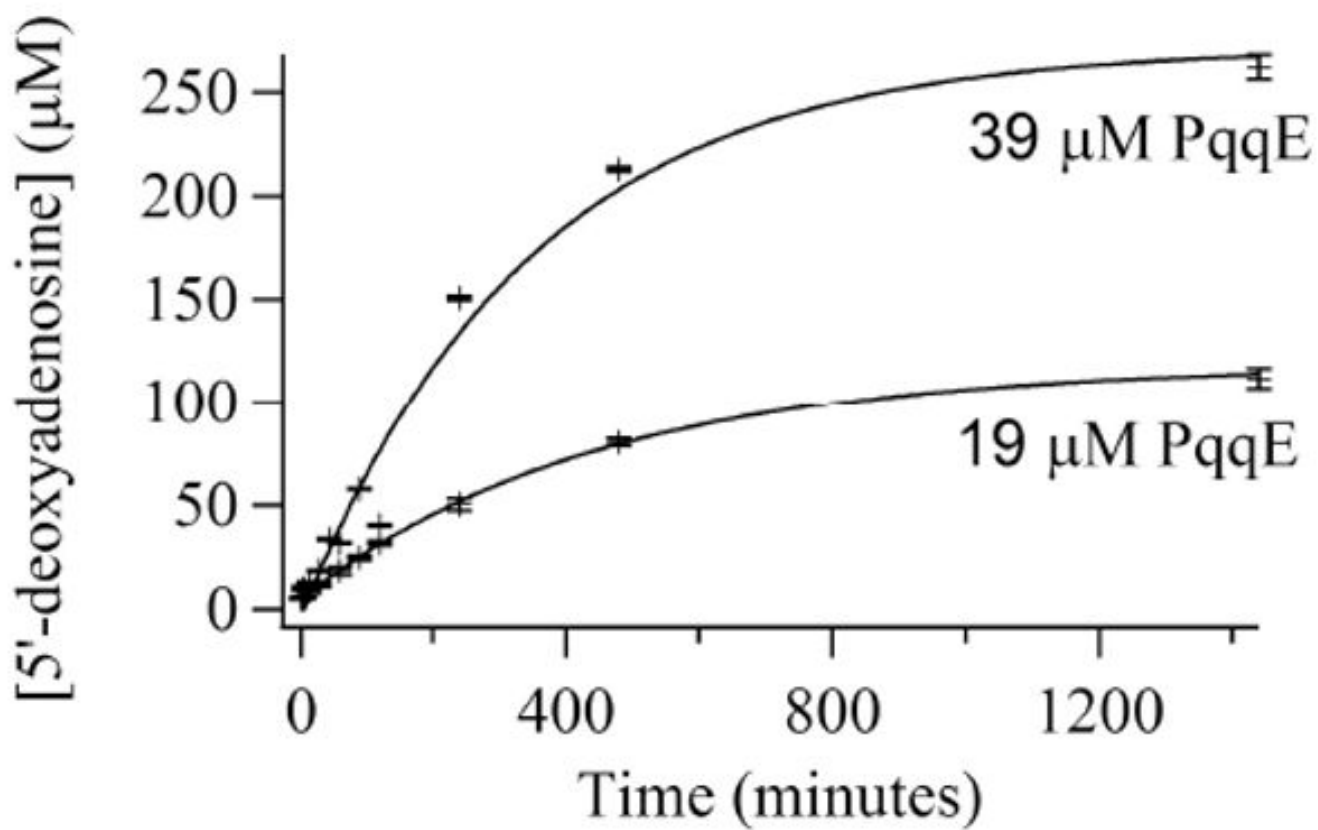


Figure 5. Time-dependent formation of 5'-deoxyadenosine from the radical SAM reaction of PqqE measured via HPLC. The black lines shown are single exponentials fitted to the data.

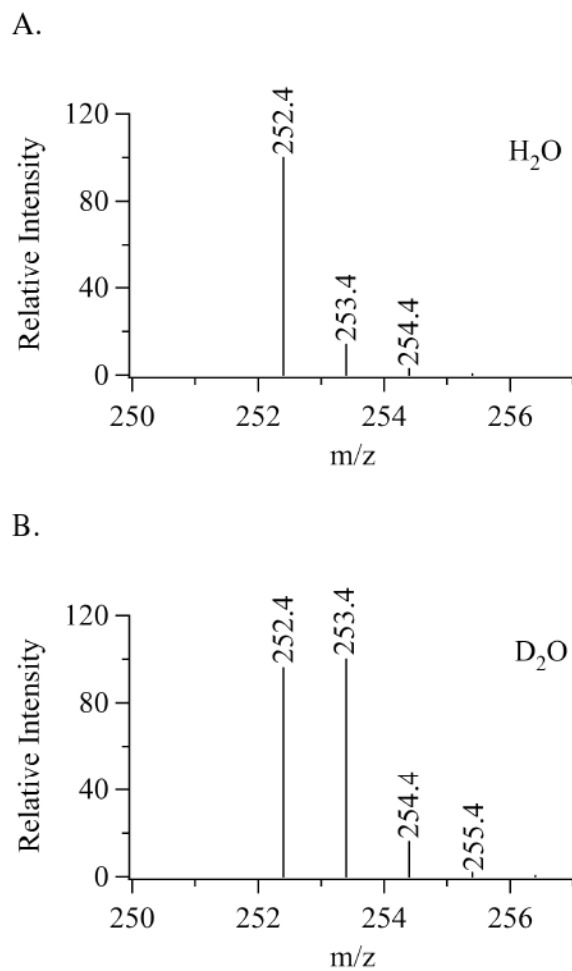
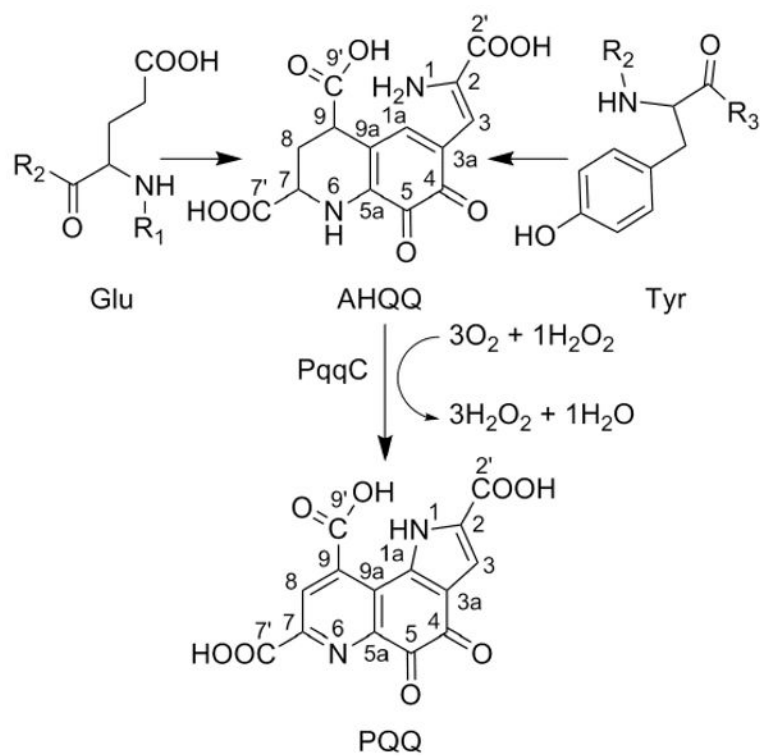
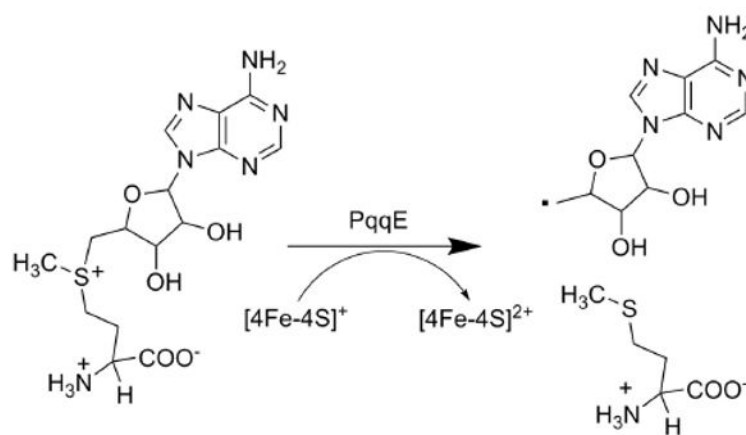


Figure 6. ESI mass spectra of the peak eluting off of the LC-MS at 28 min. **A.** Reaction done in H₂O. **B.** Reaction performed in D₂O.

**Scheme 1.**

Formation of PQQ from the fusion of glutamate and tyrosine via the intermediacy of AHQQ.

**Scheme 2.**

PqqE catalyzes the reductive cleavage of SAM to form methionine and a 5'-deoxyadenosyl radical.